Multi-organ Segmentation Using Shape Model Guided Local Phase Analysis

Chunliang Wang[1,2,3] and Örjan Smedby[1,2,3]

[1] Center for Medical Image Science and Visualization (CMIV), Linköping University, Sweden
[2] Department of Radiology and Department of Medical and Health Sciences, Linköping University, Linköping, Sweden
[3] School of Technology and Health (STH), KTH Royal Institute of Technology, Sweden

Abstract. To improve the accuracy of multi-organ segmentation, we propose a model-based segmentation framework that utilizes the local phase information from paired quadrature filters to delineate the organ boundaries. Conventional local phase analysis based on local orientation has the drawback of outputting the same phases for black-to-white and white-to-black edges. This ambiguity could mislead the segmentation when two organs' borders are too close. Using the gradient of the signed distance map of a statistical shape model, we could distinguish between these two types of edges and avoid the segmentation region leaking into another organ. In addition, we propose a level-set solution that integrates both the edge-based (represented by local phase) and region-based speed functions. Compared with previously proposed methods, the current method uses local adaptive weighting factors based on the confidence of the phase map (energy of the quadrature filters) instead of a global weighting factor to combine these two forces. In our preliminary studies, the proposed method outperformed conventional methods in terms of accuracy in a number of organ segmentation tasks.

Keywords: image segmentation, level set, local phase analysis, shape model.

1 Introduction

Automatic segmentation of anatomical structures is often needed for both clinical and epidemiological studies. As an important initial step for quantitative image analysis and data mining, the accuracy of the organ segmentation is usually one of the main factors that determine the quality of the final image analysis results. Many automated organ segmentation methods have been proposed, such as the active shape model (ASM), atlas-based methods and machine-learning-based methods [1]. No matter what framework is chosen, a crucial factor determining the segmentation accuracy is what kind of local features is used to guide the global optimization process. When dealing with medical images, methods based on the conventional image features, such as intensity and gradient, often fail to deliver satisfactory results, as the boundary between two organs may be inadequately defined due to limited resolution and intensity similarity. Even with the help of shape priors, most algorithms have difficulties in

N. Navab et al. (Eds.): MICCAI 2015, Part III, LNCS 9351, pp. 149–156, 2015.
DOI: 10.1007/978-3-319-24574-4_18

discriminating between a different organ and anatomical variation of the same organ. Local phase has been used as a robust image feature in noisy images in various image segmentation and registration applications [2–4]. However, local phase analysis is often performed using the local orientation, yielding identical local phase estimates for black-to-white and white-to-black edges. This ambiguity may mislead the segmentation when two organs' borders are too close. In this paper, we propose a model-guided local phase analysis method, where the global shape model suggests the searching orientation of the local structures. This suppresses the influence from irrelevant structures not aligned with the shape surface. Moreover, by using the gradient of the signed distance map of a statistical shape model, we can distinguish between the aforementioned two types of edges and avoid the segmentation region leaking into another organ. In addition, we propose a level-set based solution that integrates both the local-phase-based and region-based forces. Compared with previously proposed methods, the current method uses local adaptive weighting factors based on the confidence of the phase map (energy of the quadrature filters), instead of a global weighting factor, to combine these two forces. In our preliminary studies, the proposed method outperformed conventional methods in terms of accuracy for brain stripping and liver, spleen and kidney segmentation tasks.

2 Method

2.1 Quadrature Filters and Model Guided Local Phase Analysis

Quadrature filters, originally proposed by Granlund and Knutsson [5], have been successfully applied for various local structure estimation and image enhancement tasks [3, 4, 6]. The principle of these filters is to combine a ridge-picking filter with an edge-picking filter in the spatial domain. Typical 2-dimensional filter kernels are illustrated in Figs. 1a and 1b. A quadrature filter is a band-pass filter over one half of the Fourier domain. The output of this pair of filters is represented by a complex number where the output of the ridge-picking filter is seen as the real part and the output of the edge-picking filter as the imaginary part. When applied to an image, the response of ridge-like structures will be predominantly real, while the response of edge-like structures will be predominantly imaginary. The argument of this complex number in the complex plan is referred to as the *local phase* [5], θ in Fig. 1c. The magnitude (q) of the complex number is called *local energy* [5]. It is worth mentioning that local phase can also be estimated using Gabor filters where the ridge-picking filter is a sine wave multiplied with a Gaussian function, while the edge-picking filter is a cosine wave multiplied with the same Gaussian function. It is easy to see that the local phase varies when the orientation of a quadrature filter changes. To be able to produce a consistent phase map for any given image, the local phase is often estimated using the local orientation that can be estimated using either the local gradient or eigenvector decomposition of the local structure tensor. Another common way of estimating local phase is simply to combine the complex output of a set of quadrature filter pairs that evenly covers all angles in a 2D or 3D coordinate system (e.g. 4 filters in 2D and 6 filters in 3D as suggested in [5]). Notice that the combination of local phases is implicitly weighted by the local energy of those

filters, i.e. the filter with highest local energy will dominate the phase estimation. To avoid that filters with opposite relative orientation cancel out in the imaginary part (the output from an edge-picking filter will switch sign when the filter orientation inverts), Läthén et al. suggested to flip the phase along the real axis for all filters that produce a negative imaginary part [6]. This solution, just like using local orientation, will produce the same phase on black-to-white and white-to-black edges. When used for segmentation, this ambiguity could cause the organ contour to snap to the edge of a neighboring organ if the two organs' borders are too close. This scenario can very often be seen in medical images.

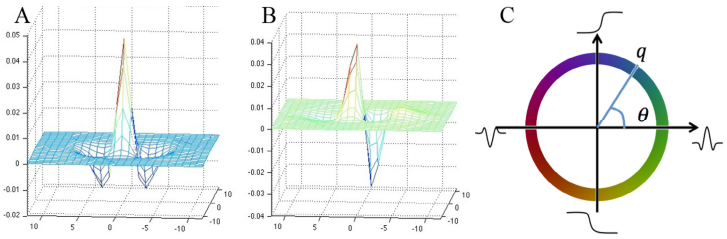

Fig. 1. An example of quadrature filter pairs in 2D. **A**, the ridge-picking filter. **B**, the edge-picking filter. **C**, The quadrature filter's response in the complex plane.

In this study, we propose to use the surface orientation of a given shape model to guide the local phase analysis. Shape models can either be mesh-based or volume-based. A review of various types of statistical shape models can be found in [7]. Nevertheless, all shape models can be converted into a signed distance map. The gradient of the the signed distance map then represents a reference orientation perpendicular to the shape surface. More importantly, the gradient also indicates which direction is inside/outside (here we assume that the distance map is positive inside and negative outside). Local phase is then estimated in the reference direction. Given a white organ on a black background, the local phase of the organ's edge should be –90°, while the local phase of a neighboring organ's edge will be 90°. Fig. 2 shows an example of applying the proposed filtering technique in a brain MRI volume. As compared with the Gaussian gradient (Fig. 2B) and the conventional quadrature filter (Fig. 2C), the energy map from the model-guided quadrature filters focus more on the edges of the skull, which is desired for skull stripping in MRI brain analysis. Compared with the phase map produced by Läthén's method (Fig. 2D), the proposed solution (Fig. 2H) delivers a more distinct pattern for identifying the inner boundary of the skull (blue) from the out surface of the brain (yellow).

As the filter orientation varies across the image, the filtering is made via local resampling by rotating a given kernel grid to align with the local reference direction. This step can also be carried out using a steerable filter, which synthesises a filter with arbitrary orientation from a linear combination of basis filters [8]. The latter may be faster if the local phase analysis needs to be performed for all pixels/voxels. However, in practice, the computation on points that are far away from the model surface can be skipped, as will be further explained in the next section.

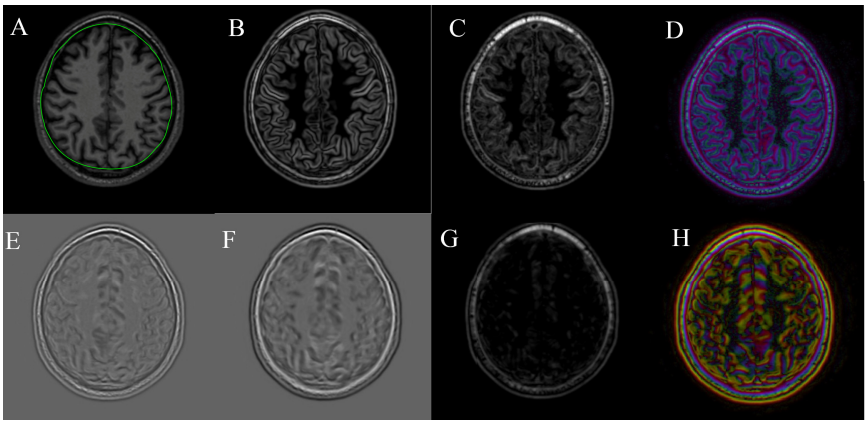

Fig. 2. A: input image, the green contour represents the cross section of the brain model; **B**: the gradient magnitude. **C, D**: local energy and phase maps using Läthén's method [6]. **E, F**, **G, H**: the real and imaginary parts of the model-guided quadrature filter and corresponding local energy and phase maps. (D, H were created using the color lookup table shown in Fig. 1C)

2.2 Integrating Region-Based and Edge-Based Energy in the Level-Set Method

To incorporate the phase information into the level set framework, we propose an energy function as described in Eq. 1, where I is the input image, and $\mathcal{R}_A$ is the segmented region. The function θ outputs the estimated local phase ($0 \le \theta < 2\pi$) at any given location. τ is an input parameter defining the targeted phase (e.g. $\pi/2$ for a black-to-white edge and $3\pi/2$ for a white-to-black edge).

$$E(\partial\mathcal{R}) = \int_0^1 g\left[\theta\left(I\left(\partial\mathcal{R}_A(c)\right)\right) - \tau\right]^2 |\mathcal{R}_A(c)|dc \tag{1}$$

The function g is a simple period-fixing function that ensures that the phase difference between θ and τ is measured in the range from $-\pi$ to π (Eq. 2).

$$g(\delta) = \begin{cases} \delta & if\ -\pi < \delta \le \pi \\ \delta - 2\pi & if\ \delta > \pi \\ \delta + 2\pi & if\ \delta \le -\pi \end{cases} \tag{2}$$

Notice that Eq. 1 is very similar to the conventional geodesic active contours, except that $\theta(I)$ replaces∇I, and the period-fixing function g replaces the gradient magnitude inverse function. Similar to the conventional geodesic active contours, the force of this phase-based energy function vanishes in flat areas where the quadrature filters cannot pick up any signals. To overcome this problem and guide the contour's movement even far away from any borders, we propose an integrated energy function that combines the phase-based energy and the region-based energy:

$$E(\partial\mathcal{R}) = \alpha \int_0^1 g\left[\theta\left(I\left(\partial\mathcal{R}_A(c)\right)\right) - \tau\right]^2 |\mathcal{R}_A(c)|dc - \int_{\mathcal{R}_A}\int w(x,y)\log\left[p_A\left(I(x,y)\right)\right]dxdy\ -$$
$$\int_{\mathcal{R}_B}\int w(x,y)\log\left[p_B\left(I(x,y)\right)\right]dxdy \tag{4}$$

Here, p_A and p_B are the probability functions of a given pixel/voxel falling into region A or B. In the case of medical images, their distributions could be learned either from statistical analysis of image databases, or on the fly using preliminary segmentation results. Function w is a weighting function that weights the fitting energy using the local energy output (q) from the quadrature filter, as described by Eq. 5:

$$w(x,y) = \frac{1}{1+q(I(x,y))} \tag{5}$$

Eq. 4 can be minimized by solving the following descent equation:

$$\frac{\partial \phi}{\partial t} = \left[\alpha g(\theta-\tau)^2 \mathrm{div}\left(\frac{\nabla\phi}{|\nabla\phi|}\right) + \alpha g(\theta-\tau) + w\log(p_B) - w\log(p_A)\right]|\nabla\phi| \tag{6}$$

Here, ϕ is the level set function, which is a signed distance map from the contours. The last 3 components on the right side can be seen as a group of external forces. Fig. 3 shows an example of a liver segmentation case, in which the phase-based term, the region-based terms and their combination are visualized side by side. In practice, we simplify the first component on the right side by replacing it with $\beta\mathrm{div}(\nabla\phi/|\nabla\phi|)$, where β is a weighting factor, as it is just a regulation term that corresponds to the curvature force in the conventional level set methods. By plugging the model term into the formulation, we arrive at the final speed function given below:

$$\frac{\partial \phi}{\partial t} = \left[\beta\mathrm{div}\left(\frac{\nabla\phi}{|\nabla\phi|}\right) + \alpha g(\theta-\tau) + w\log(p_B) - w\log(p_A) + m(t)\right]|\nabla\phi| \tag{7}$$

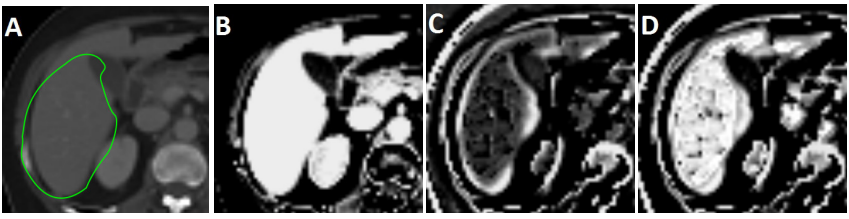

Fig. 3. A. An axial view of an input volume (green contour: the current shape model), **B**. The region-based speed terms based on the image intensity. **C** The phase-based term estimated using the model **D**. The combined external speed map. Notice that the connection between liver and kidney is removed.

To propagate the level set function according to the speed function above, we adapted a coherent propagating level set algorithm proposed in [9, 10]. This method is able to detect the convergence of the level set function. Note that, given a contour starting from the current best fitting model, the statistical model and its corresponding phase map only need to be updated if the contour has moved a certain distance from the current model. As pointed out in [10], it is possible to design a model term that limits the zero level to stay in a narrow band with fixed width (e.g. 3mm) around the previous model. This means that before the contour reaches convergence within this narrow band, the statistical model does not need to be updated. Given a good initialization, the model fitting and the corresponding local phase map regeneration are only repeated a small number of times (<20) throughout the whole segmentation process.

Moreover, since the contour is not allowed to move beyond the narrow band, we only need to compute the local phase map for the points located on the narrow band.

2.3 Hierarchical Segmentation Pipeline and Multi-scale Phase Analysis

To segment multiple organs in full-body CT datasets, we implemented a hierarchical segmentation pipeline, similar to the work of Wang et al. [10]. First, the unseen full body CT volume is registered to a standard patient selected from a set of training data. Then we sequentially segment the ventral cavity, thoracic cavity, abdominal cavity, lungs, liver, spleen, kidneys and bladder. All segmentation steps are made using the proposed method described in section 2.2. The segmentation of the higher-level structures provides an estimated position for the lower level structures for initializing the model-based segmentation. For a non-enhanced CT dataset, the boundary information from higher-level structures, such as the abdominal cavity, also constrains the segmentation of the lower-level structures. However, for enhanced CT, this constraint is removed, thanks to the phase-based energy, which can reliably detect the organ's boundary and avoid the leaking problem in most cases. In addition to the anatomical hierarchy, we also perform the segmentation in a coarse-to-fine resolution hierarchy. All structures are first segmented at 3.5mm isotropic resolution, and then the segmentation of the lower level organs is repeated at 2mm and finally at the input resolution, which is about 0.8×0.8×1.5mm. At each resolution, we used the same 7×7×7voxel quadrature filter, which implies that the local phase analysis is done at different scales (in millimeters). This strategy helps to gradually attract the contour towards the organ border, even if the initial shape model is a bit away from the ideal position.

3 Experiments and Results

To validate the proposed model-guided phase analysis method, we first compared it with the multi-scale phase analysis method proposed in [6] (both put into the integrated phase- and region-based level set framework described in section 2.2) and with the conventional integrated gradient and region-based method [11] for skull stripping in MRI. Publicly available data from the brain segmentation challenge site (http://mrbrains13.isi.uu.nl/) was used. The segmentation accuracy on 5 training datasets is 96.3±1.6% with the gradient- and region-based method, 95.8±2.5% with the multi-scale phase based approach and 97.8±1.4% with the proposed method (mean Dice coefficient ± SD). Results on test datasets are not available as the current implementation cannot provide the white matter and gray matter segmentation required by the website.

The proposed method was further tested for multi-organ segmentation using the data from the Visceral multi-organ segmentation challenge [12]. Our method was trained using 7 non-enhanced CT (CT) and 7 contrast-enhanced CT (CECT) datasets and tested on 8 non-enhanced and 10 enhanced CT datasets. For testing, the participants submitted a virtual machine with their segmentation software installed, and the organizer ran the program against the unseen testing data. This prevents the teams

from training their methods on the testing data by visually checking the segmentation results. The proposed method outperformed other methods in liver segmentation and kidney segmentation. Detailed results and comparison with previous leading methods are listed in Table 1. The average processing time for segmenting all 6 major organs is about 30 minutes on a PC with Intel i7 (1.9GHz). A 7×7×7 quadrature filter with a central frequency of $\pi/2$ and a bandwidth of 6 octaves was used for the experiments.

Table 1. Multi-organ segmentation in CT and CECT datasets (mean Dice coefficient)

Data	Method	Liver	Right Kidney	Left Kidney	Spleen	Right Lung	Left Lung
CT (8 cases)	Toro et al.[13]	86.6%	79.0%	78.4%	70.3%	**97.5%**	**97.2%**
	Vincent et al. [12]	93.4%	**92.5%**	86.6%	–	97.0%	97.0%
	Wang et al.[10]	93.4%	90.4%	87.3%	**91.3%**	96.2%	96.0%
	Proposed method	**93.6%**	79.6%	**89.6%**	91.0%	97.0%	96.1%
CECT (10 cases)	Toro et al. [13]	88.7%	88.9%	91.0%	73.0%	96.3%	95.9%
	Vincent et al. [12]	94.2%	92.7%	94.3%	–	**97.4%**	96.9%
	Wang et al.[10]	93.0%	92.9%	93.0%	87.4%	96.6%	96.7%
	Proposed method	**94.9%**	**95.9%**	**94.5%**	**90.9%**	97.1%	**97.2%**

4 Discussion and Conclusion

Shape priors have been adapted in a large variety of image segmentation tasks. However, most existing methods focus on using local image features to update the global shape model and on using the global shape model to regularize the propagation of the segmentation contour/mesh. Very few studies have suggested using the estimated global shape to guide the local feature analysis. To some extent, the proposed method is similar to Zheng et al.'s machine learning based method for heart chamber segmentation [1], where steerable features are used to guide the deformation of an ASM. However, the implementation of using the local phase is more general, as the filter need not be trained for each special type of data, except for choosing a proper target phase τ. In contrast to conventional gradient-based level sets, using model-guided phase analysis can not only attract the contour to the organ edges, but also make it favor a certain type of edges and repel from the edges of a neighboring organ. In addition, local phase is intensity-invariant, which makes it better suited for medical images with inhomogeneity. Although the phase computation is more time-consuming than the gradient, as pointed out in section 2.2, the process needs only to be repeated a small number of times when combined with coherent propagation. Compared to geodesic active contours, which use an advection force (corresponding to the second order derivative of the input image) that needs to be computed in each iteration of the level set propagation, the model-guided local phase analysis could even be favorable in terms of speed.

The integrated energy function presented above is inspired by Paragios' et al. work in [11]. However, instead of using a global weighting factor, we propose a local weighting scheme. This helps to suppress the influence of the intensity-based terms in

areas where two organs are close to each other and to let the phase map take more responsibility for delineating the boundary in such cases.

A limitation of the model-guided phase analysis method is that it requires the shape model to be relatively well positioned initially. Large offset from the target may confuse the contour propagation. For example, in our Visceral challenge experiment, the right kidney model initialization was poor in one of the eight CT cases that leading to total failure of the segmentation and explaining the inferior mean Dice coefficient presented in Table 1. It is possible that the machine learning based organ detection and pose estimation proposed in [1] could be a good solution to this issue.

In conclusion, a model-based segmentation framework using model-guided local phase analysis is proposed. By using the surface orientation of the shape model as a reference direction, the proposed method could distinguish between black-to-white and white-to-black edges and avoid the segmentation region leaking into neighboring organs. In our preliminary studies, the proposed method outperformed some conventional methods in a number of single-organ and multi-organ segmentation tasks.

References

1. Zheng, Y., Barbu, A., Georgescu, B., Scheuering, M., Comaniciu, D.: Four-chamber heart modeling and automatic segmentation for 3-D cardiac CT volumes using marginal space learning and steerable features. IEEE Trans. Med. Imaging 27, 1668–1681 (2008)
2. Knutsson, H., Andersson, M.: Morphons: segmentation using elastic canvas and paint on priors. In: IEEE International Conference on Image Processing, pp. II–1226–9 (2005)
3. Belaid, A., Boukerroui, D., Maingourd, Y., Lerallut, J.-F.: Phase-Based Level Set Segmentation of Ultrasound Images. IEEE Trans. Inf. Technol. Biomed. 15, 138–147 (2011)
4. Wang, C., Smedby, Ö.: Model-based left ventricle segmentation in 3d ultrasound using phase image. Presented at the MICCAI Challenge on Echocardiographic Three-Dimensional Ultrasound Segmentation (CETUS), Boston (2014)
5. Granlund, G.H., Knutsson, H.: Signal Processing for Computer Vision. Kluwer Academic Publishers (1994)
6. Läthén, G., Jonasson, J., Borga, M.: Blood vessel segmentation using multi-scale quadrature filtering. Pattern Recognit. Lett. 31, 762–767 (2010)
7. Heimann, T., Meinzer, H.-P.: Statistical shape models for 3D medical image segmentation: A review. Med. Image Anal. 13, 543–563 (2009)
8. Freeman, W.T., Adelson, E.H.: The design and use of steerable filters. IEEE Trans. Pattern Anal. Mach. Intell. 13, 891–906 (1991)
9. Wang, C., Frimmel, H., Smedby, Ö.: Fast Level-set Based Image Segmentation Using Coherent Propagation. Med. Phys. 41, 073501 (2014)
10. Wang, C., Smedby, Ö.: Automatic multi-organ segmentation in non-enhanced CT datasets using Hierarchical Shape Priors. Proceedings of the 22nd International Conference on Pattern Recognition (ICPR). IEEE, Stockholm (2014)
11. Paragios, N., Deriche, R.: Geodesic active regions and level set methods for supervised texture segmentation. Int. J. Comput. Vis. 46, 223–247 (2002)
12. Visceral Benchmark, `http://www.visceral.eu/closed-benchmarks/anatomy2/anatomy2-results/`
13. del Toro, O.A.J., Müller, H.: Hierarchic Multi–atlas Based Segmentation for Anatomical Structures: Evaluation in the VISCERAL Anatomy Benchmarks. In: Menze, B., Langs, G., Montillo, A., Kelm, M., Müller, H., Zhang, S., Cai, W.(T.), Metaxas, D. (eds.) MCV 2014. LNCS, vol. 8848, pp. 189–200. Springer, Heidelberg (2014)